About the role of Westerly Wind Events in the possible development of an El Niño in 2014

Christophe E. Menkès, Matthieu Lengaigne, Jérôme Vialard, Martin Puy, Patrick Marchesiello, Sophie Cravatte, Gildas Cambon

AGU PUBLICATIONS

Geophysical Research Letters

RESEARCH LETTER
10.1002/2014GL061186

Key Points:
- Westerly wind events were crucial in the development of the 1997 El Niño
- Early 2014 conditions looked like 1997 but westerly wind activity stopped
- This lack of events after April 2014 prevented an El Nino like 1997

Supporting Information:
- Readme
- Figure S1

Correspondence to:
C. E. Menkes,
Christophe.Menkes@ird.fr

Citation:
Menkes, C. E., M. Lengaigne, J. Vialard, M. Puy, P. Marchesiello, S. Cravatte, and G. Cambon (2014), About the role of Westerly Wind Events in the possible development of an El Niño in 2014, *Geophys. Res. Lett.*, *41*, 6476–6483, doi:10.1002/2014GL061186.

Received 11 JUL 2014
Accepted 7 SEP 2014
Accepted article online 11 SEP 2014
Published online 26 SEP 2014

About the role of Westerly Wind Events in the possible development of an El Niño in 2014

Christophe E. Menkes[1,2], Matthieu Lengaigne[2,3], Jérôme Vialard[2], Martin Puy[2], Patrick Marchesiello[4], Sophie Cravatte[1,4], and Gildas Cambon[4]

[1]Centre IRD, Nouméa, New Caledonia, [2]LOCEAN Laboratory, IPSL, Sorbonne Universités (UPMC, Université Paris 06)-CNRS-IRD-MNHN, Paris, France, [3]Indo-French Cell for Water Sciences, IISc-NIO-IITM–IRD Joint International Laboratory, NIO, Goa, India, [4]IRD/LEGOS Laboratory, Toulouse, France

Abstract Similarities between early 1997 and 2014 has prompted climate scientists to wonder if an El Niño matching the 1997 "El Niño of the century" could develop in 2014. Until April 2014, the equatorial Pacific exhibited positive heat content anomalies along with an eastward warm pool displacement similar to those found during the onset of strong El Niño events. Yet in July 2014, the warm pool had retreated back to its climatological positions and equatorial temperature anomalies were much weaker than in mid-1997. Dedicated oceanic simulations reveal that these weak interannual anomalies can be attributed to differences in Westerly Wind Event (WWE) sequences. In contrast with 1997, the lack of WWEs from April to June significantly limited the growth of eastern Pacific anomalies and the eastward warm pool displacement in 2014. With the absence of additional WWE activity, prospects for a mature El Niño in late 2014 are fading.

1. Introduction

The El Niño–Southern Oscillation (ENSO) that develops in the tropical Pacific is the dominant mode of climate variability at interannual timescales, with massive global socioeconomic impacts [e.g., *McPhaden et al.,* 2006a]. ENSO grows as the result of the Bjerknes feedback [*Bjerknes*, 1969], a positive feedback between the ocean and atmosphere. Its termination is the result of a delayed negative feedback associated with Sverdrup and equatorial wave dynamics [*Wang and Picaut*, 2004]. Favorable grounds are needed for the Bjerknes feedback to result into a full-fledged El Niño. The equatorial Pacific warm water volume (WWV, or equivalently upper ocean heat content) is considered to be a good El Niño predictor [*Meinen and McPhaden*, 2000] (although less efficient in recent years [*McPhaden*, 2012]) with anomalously high heat content during the early part of the El Niño years (Figure 1a).

For a given equatorial heat content anomaly, the ENSO cycle, however, exhibits considerable irregularity in its onset timing, amplitude (Figure 1b) and spatial structure. Both dynamical and statistical ENSO forecasts experience a spring prediction barrier for El Niño onset and ENSO amplitude forecasts remain challenging [e.g., *Barnston et al.,* 2011; *Clarke*, 2014]. High-frequency wind variability plays an important role in El Niño evolution [e.g., *Boulanger et al.,* 2004; *McPhaden et al.,* 2006b; *Wang et al.,* 2011]. Part of this high-frequency wind forcing occurs as Westerly Wind Events (WWEs) over the western and central Pacific [*Harrison and Vecchi*, 1997] and is modulated by ENSO-related warm pool displacements [e.g., *Eisenman et al.,* 2005; *Seiki and Takayabu*, 2007]. WWEs trigger eastward currents that shift the warm pool eastward dramatically and generate equatorial downwelling oceanic Kelvin waves that deepen the thermocline in the central and eastern equatorial Pacific [e.g., *Lengaigne et al.,* 2004b]. Both of these processes induce a positive atmospheric retroaction favoring the onset and developments of El Niño events [*Lengaigne et al.,* 2003]. As a result, WWE strength and distribution modulate the strength or timing of El Niño events and contribute to ENSO irregularity [*Gebbie et al.,* 2007; *Lopez et al.,* 2013; *Lian et al.,* 2014].

The 1997/1998 El Niño was referred to as the "El Niño of the (last) century" [*McPhaden*, 1999]. It was characterized by an exceptional eastward shift of the warm pool and related atmospheric convection into the eastern equatorial Pacific [*McPhaden*, 1999; *Cai et al.,* 2014]. The strongest on-record recharged oceanic heat content and the occurrence of a series of WWEs with a strong WWE in March 1997 (Figures 1a and 2a) have been invoked for explaining the unusually large amplitude of that El Niño event [*Boulanger et al.,* 2004; *Lengaigne et al.,* 2004a]. The WWV was also anomalously high in early 2014, and two relatively strong WWEs

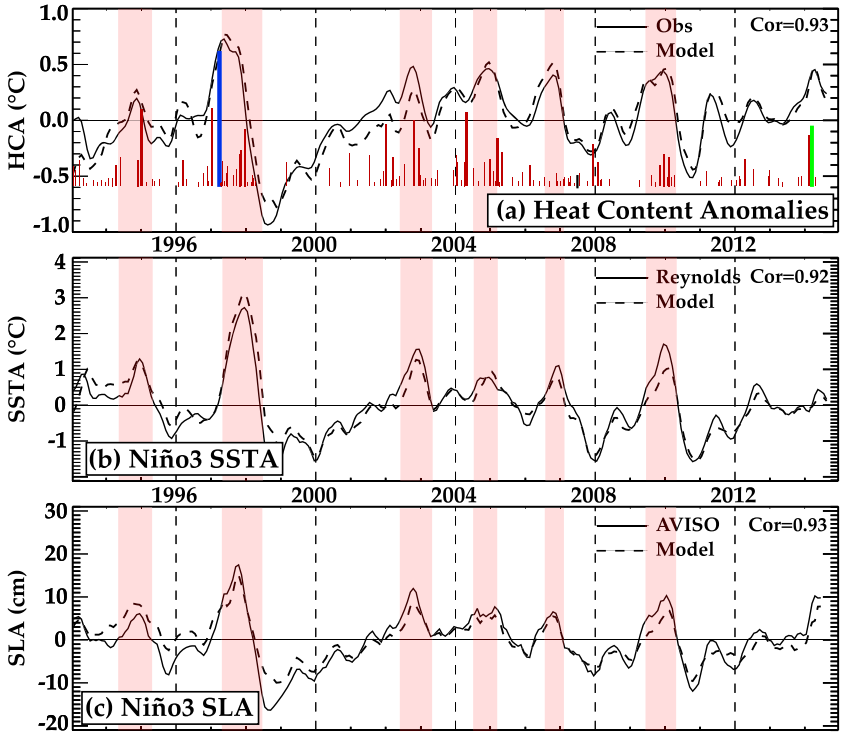

Figure 1. Time series of (a) equatorial Pacific heat content anomalies (HCA), (b) Niño3 sea surface temperature anomalies (SSTA), and (c) Niño3 sea level anomaly (SLA) over the 1993–2014 period for the observations (continuous lines) and REF experiment (dotted lines). The Pearson correlation ($p < 0.01$) between modeled and observed time series is indicated on the upper right of each panel. Red bars normalized to their 1993–2014 maximum (the march 1997 WWE) in Figure 1a indicate WWEs, with the length of the bar proportional to the space-time integral of WWE zonal stress anomalies (this a good measure of the equatorial wind effects on the ocean dynamics in the 3°S–3°N band [*Kessler et al.*, 1995]). The bar widths are proportional to the WWE durations. The March 1997 WWE is indicated in blue and the February–March 2014 WWE is indicated in green. The pink shading illustrates the periods considered as El Niños based on http://www.cpc.ncep.noaa.gov/products/analysis_monitoring/ensostuff/ensoyears.shtml.

occurred in the western Pacific in February and March (Figures 1a and 2b). Those WWEs started pushing the warm pool eastward and triggered a strong downwelling Kelvin wave (Figure 2b). These similarities with early 1997 led climate scientists to wonder if this event would rival the catastrophic 1997–1998 El Niño event [*Tollefson*, 2014]. However, one must keep in mind that not all strong WWE sequences result in the development of extreme El Niño events [*Lengaigne et al.*, 2004a; *Fedorov et al.*, 2014; *Lian et al.*, 2014]. Understanding reasons behind the diversity of ENSO response to WWE forcing thus remains an important question to improve our understanding of ENSO predictability.

The present paper aims at characterizing similarities and differences between the equatorial Pacific Ocean state in early 1997 and 2014. We will discuss the specific role of WWEs in this evolution using both observations and ocean model experiments. Our intention is also to put the equatorial Pacific conditions of early 2014 in perspective by comparing them with those associated with moderate and strong El Niño events over the past three decades and to discuss the likelihood for a strong El Niño event in late 2014.

2. Data and Method

The "observed" data sets (hereafter OBS) used in this study include *Reynolds and Smith* [1994] sea surface temperature (SST) data, National Centers for Environmental Prediction/Department of Energy Global Reanalysis 2 (NCEP2) [*Kanamitsu et al.*, 2002] surface meteorological data, Archiving, Validation, and Interpretation of Satellite Oceanographic (AVISO) data (www.aviso.oceanobs.com/fr/accueil/index.html) sea level anomalies, Ocean Surface Current Analyses-Real (OSCAR) time surface currents [*Bonjean and Lagerloef*, 2002; www.oscar.noaa.gov] and equatorial Pacific heat content anomalies (hereafter HCA) derived from

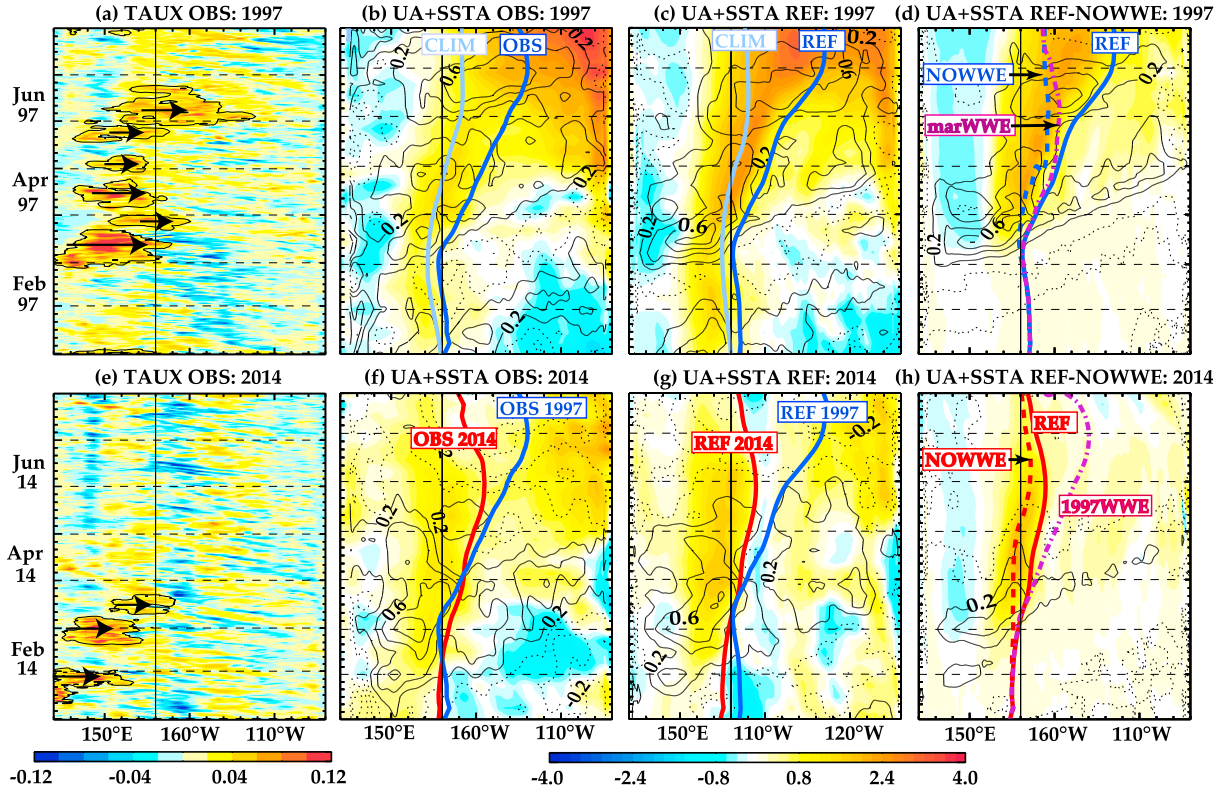

Figure 2. January–July 1997 3°N–3°S zonal time section of (a) zonal wind stress referred to as TAUX anomalies (colors with observations (OBS) referring to the NCEP2 model forcing) and WWEs (contours) and SST (color), surface currents (thin black contours) anomalies for (b) observations, (c) REF experiment, and (d) REF minus NOWWE experiments. (e–h) Same as Figures 2a–2d but for 2014. Plain blue lines indicate the EEWP position defined as the longitudinal position of the 28.5°C isotherm in the 3°S–3°N band. Plain grey lines indicate the climatological position of the EEWP. In Figure 2d, the dashed blue (respectively, dash-dotted purple) line indicates the EEWP position for the NOWWE (respectively, MarWWE) experiments. In Figures 2f and 2g, the EEWP is indicated in blue for 1997 and in red for 2014. In Figure 2h, the dashed red (respectively, dash-dotted purple) line indicates the EEWP position for the NOWWE (respectively, 1997WWE) experiments. Labels of the experiment EEWP are added for clarity on each panel.

averaged temperature anomalies over the first 300 m within 5°N and 5°S (the T300 product on http://www.pmel.noaa.gov/tao/elnino/wwv/). This product is based on data from moored buoys, expendable bathythermographs, and Argo floats. It is believed that the numerous Argo profiles partially compensate the failure of many moorings since 2012 and that the quality of the HCA analysis has not decreased too much since then (M. McPhaden, personal communication, 2014). SST, NCEP2, and T300 data cover 1980–2014 while the sea level and currents data cover 1993–2014. Anomalies are obtained by removing the 1993–2013 climatological seasonal cycle. El Niño events are defined as the December-January-February (DJF) averaged value of the Niño 3.4 (5°N-5°S, 120°W-170°W) 3-month filtered SST anomaly greater than 0.5°C (see http://www.cpc.noaa.gov/products/analysis_monitoring/ensostuff/ensoyears.shtml).

The Regional Oceanic Modeling System (ROMS) [*Shchepetkin and McWilliams*, 2005] is employed to explore the WWE impact in 1997 and 2014. Our configuration extends over the tropical Pacific region (35°S–35°N, 110°E–80°W) with a one-fourth horizontal resolution. It has 41 terrain-following vertical levels leading to a vertical resolution of 2 to 5 m within 50 m of the ocean surface and 10 to 20 m in the thermocline. Open boundary conditions are specified using the climatology of a global model simulation as in [*Jullien et al.*, 2012]. The model time step is 1 h. The initial state of the experiments described below is taken as the last time step of *Jullien et al.* [2014] 10 years model spin up using climatological forcing from ERS1–2 stress and Comprehensive Ocean-Atmosphere Data Set (COADS) freshwater and heat flux climatologies.

Six-hourly heat, fresh, and momentum fluxes used to force the reference model simulation are calculated using [*Fairall et al.*, 1996] bulk formulae with NCEP2 surface atmospheric inputs. After the 10 year spin up, the reference simulation (hereafter REF) is performed from January 1993 to end of July 2014. From the 1993–2013 seasonal cycle, we calculated seasonal anomalies of equatorial Pacific heat content, SST and sea level

anomalies in the Niño3 region [90°W–150°W, 5°S–5°N]. These agree very well with the observed ones, with correlation of 0.93, 0.92, and 0.93, respectively (Figure 1). Note that the SST agreement is not unexpected as the flux specification introduces a restoring to observed near surface atmospheric temperature. To compare the oceanic impact of the WWEs during 1997 and 2014, we first isolated so-called "WWEs" as follows. Zonal stress seasonal (referred to as TAUX) anomalies in the 5°S–5°N band were calculated and regions with anomalies greater than 0.05 N m^{-2} over 10° longitude and lasting more than 5 days were labeled as WWEs (contours in Figures 2a and 2e and in Figure S1 in the supporting information). Note that such criteria are about twice stricter than those used in *Harrison and Vecchi* [1997]. A 6-hourly NOWWE stress field was then produced by zeroing the WWE regions in the stress seasonal anomaly field (this results in only keeping the stress seasonal cycle within WWEs) and by applying a smooth transition in space and time to prevent spurious jumps in the NOWWE stress. With these choices of thresholds six major events are selected as WWE entities before mid-1997 with two particularly strong and long-lasting events in March and April 1997 (see Figure 2a and bars and caption of Figure 1a) and only three events in 2014 with two stronger WWEs in mid-January and February and March 2014 (Figures 1a and 2e). Sensitivity tests with a weaker amplitude threshold (0.02 N m^{-2}) for WWE identifications did not change the main conclusions of the present study (not shown). Heat fluxes and fresh water fluxes from the REF experiment are applied in the NOWWE experiment, so that only the dynamical effect of WWEs is removed in NOWWE. We also performed two other sensitivity experiments. In the MarWWE experiment, the March 1997 WWE is applied while other WWEs that occurred later in 1997 were removed as in NOWWE. Lastly, in the 1997WWE experiment, all WWEs of 1997 were added to the NOWWE stress in 2014. The zonal wind forcing used in all experiments is shown in Figure S1 in the supporting information.

3. Results

Figure 2 displays the observed equatorial Pacific evolution during the onset and growth of the 1997 El Niño (Figures 2a and 2b) and during early 2014 (Figures 2e and 2f). The March 1997 WWE (Figure 2a) is followed by a rapid eastward displacement of the eastern edge of the warm pool (EEWP, defined as the 28.5°C isotherm), which translates into a warming west of the EEWP (Figure 2b). This WWE also initiates a strong downwelling Kelvin wave, evident in the surface current signal, that reaches the eastern Pacific in early May, triggering a rapid surface warming (Figure 2b). This WWE is followed by other WWEs from April to June 1997, which are associated with a prolonged eastward displacement of the EEWP until early July, with intense surface jets over the warm pool and sustained SST anomalies in the central and eastern Pacific.

Two major WWE and a weaker event occurred in late January, in early, and mid-February 2014 (Figure 2e). These events initiated a strong surface jet over the warm pool, a downwelling Kelvin wave and a warming in the eastern Pacific in early May (Figure 2f). They were followed by a rapid eastward displacement of the EEWP and a warming in the central Pacific. Although early 1997 and 2014 display a qualitatively similar evolution early in the year, differences are evident in their late May oceanic state: (1) the EEWP only reached 155°W in 2014 compared to 140°W in 1997 (thick red and blue lines of Figure 2f), (2) the warming in the central and eastern Pacific in 2014 (Figure 2f) was half of that in 1997 (Figure 2c), and (3) no other WWEs occurred after March 2014 (Figure 2e) in contrast with 1997 (Figure 2a). The equatorial Pacific evolution between these two periods further diverged in summer, with a seemingly dying event in 2014 characterized by an EEWP retreating from June onward back to its climatological position and with mild eastern Pacific SST anomalies at the end of July 2014. Conversely, from June 1997, the El Niño continued to grow into a strong and mature event until the end of the year.

During these two periods, the model SST and surface currents evolutions agree well with observations described above, both in terms of timing and amplitude (Figures 2b and 2c and Figures 2f and 2g). Strong eastward surface jets near the EEWP indeed induce its rapid eastward shift mostly via horizontal advection (not shown), with zonal advection and the resulting SST anomaly being larger in May 1997 than in May 2014 (Figure 2g). To investigate the exact influence of the WWE sequences in early 1997 and 2014, we compare the REF experiment anomalies with the difference between REF and NOWWE during these two periods (Figures 2c and 2d and 2g and 2h). The REF-NOWWE panels clearly illustrate that the warming around the dateline and the related eastward displacement of EEWP are strongly linked to the WWE sequence. Half of the EEWP displacement in late April 1997 can be attributed to the WWEs that occurred over the warm pool (compare dashed and plain blue curves of Figure 2d with grey curves on Figure 2c), while almost all of the subsequent EEWP displacement until July 1997 is linked to the subsequent WWE developments. In 2014,

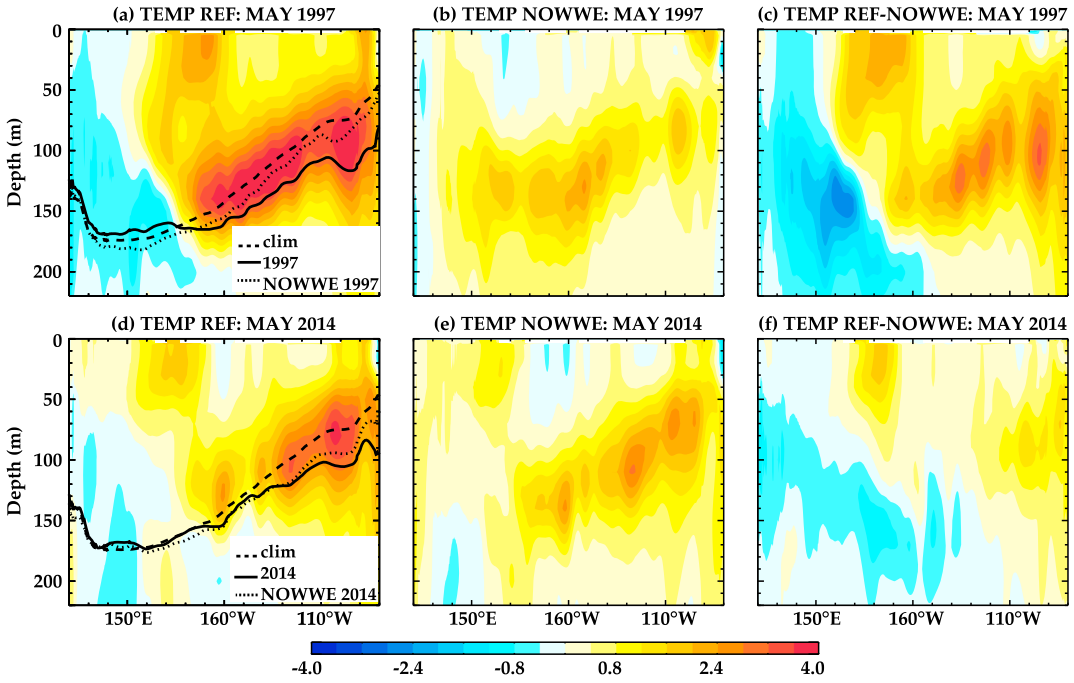

Figure 3. 3°N–3°S section of May 1997 temperature anomalies with respect to the seasonal cycle from the (a) REF, (b) NOWWE, and (c) REF minus NOWWE experiments. Thick curves in Figure 3a indicate the thermocline depth for climatology (dashed), REF (plain), and NOWWE (dotted). (d–f) Same for May 2014. Labels for thermocline depths have been added for clarity.

almost all of the EEWP displacement is linked to the WWEs with the NOWWE situation being similar to climatology (compare grey curves of Figure 2c and red curves of Figure 2h).

During the two 1997 and 2014 January–May periods, the ocean responded to WWEs locally with strong eastward surface jets advecting the EEWP eastward. However, while these jets persisted until July in 1997 under the development of additional WWEs (Figures 2b–2d), they vanished in early May in 2014 (Figures 2f–2h), most likely because of the absence of significant WWE forcing from April 2014 onward (Figure 2d). As a result the April-May EEWP eastward displacement was weaker in 2014 than in 1997 (Figures 2f and 2g). The MarWWE allows to further assessing the role of WWEs after March 1997. When WWEs occurring after March 1997 are omitted, the EEWP position in late May 1997 is very similar with the NOWWE experiment and closer (~1000 km east) to the EEWP position in 2014. The EEWP in MarWWE experiment finally retreats back toward its climatological position in late July (Figure 2d). This experiment clearly demonstrates that, while the March 1997 WWE was responsible for most of the EEWP displacement until the end of April, the subsequent WWEs largely contributed to further push the warm pool eastward later in 1997. These experiments suggest that although weaker than the March 1997 WWE, the subsequent WWEs in April and June 1997 were essential in sustaining the eastward displacement of the warm pool during spring and summer and strongly contribute to the onset and fast growth of the 1997 El Niño event. Finally, using the 1997WWE, we tested whether differences in EEWP displacements between 1997 and 2014 are linked to WWE characteristics, or to differences in background conditions such as oceanic stratification, or winds outside of the warm pool. Adding the 1997 WWE sequence in 2014 results in a similar eastward displacement of the EEWP in 2014 and 1997 until mid-June (purple line in Figure 2h). It then retreats back toward the west under the occurrence of strong easterly anomalies in the central Pacific in June and July (Figure 2e).

Figure 3 further illustrates the contribution of the integrated WWE impact on the equatorial upper ocean temperature anomalies in May, a month when the 1997 and 2014 Pacific evolutions are strongly diverging and the 2014 EEWP retreats back to the west. Maximum temperature anomalies during both years are located along the climatological thermocline position (Figures 3a and 3d). These anomalies are considerably larger in 1997 than in 2014, especially in the central Pacific where they reach 4°C against ~1.5°C in 2014. This results in deeper thermocline anomalies in May 1997 than in May 2014. The NOWWE experiment anomalies (Figure 3b) allow to isolate the contribution of the background wind, while the REF minus NOWWE

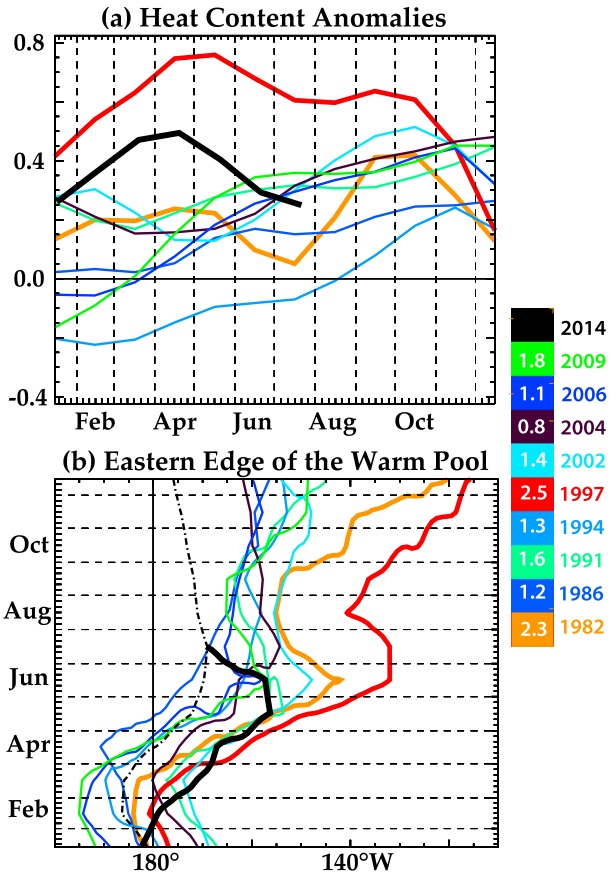

Figure 4. (a) Observed time series of 5°N–5°S Pacific HCA for all 1980–2014 El Niño years. (b) Idem but for the position of the EEWP. The curve colors correspond to the years indicated on the left of the color table). Thick colored lines represent the two major El Niño 1982 and 1997 and the thick black line is the 2014 situation. The colors ranging from black, blue, green, and red (rainbow like) indicate increasing values of the El Niño event amplitude at their peak (DJF). These values are noted in white in the color table and taken from http://www.cpc.ncep.noaa.gov/products/analysis_monitoring/ensostuff/ensoyears.shtml. The dash-dotted line in Figure 4b indicates the EEWP climatological position.

anomalies (Figure 3c) isolate the effect of WWEs on anomalous temperature signals. During both periods, anomalies associated with the background wind signals are of the same magnitude. In contrast, WWE-related temperature anomalies are considerably larger in 1997 (Figure 3c) than in 2014 (Figure 3f) and dominate the total warming signal (Figure 3a). The WWE-related impact therefore results in a 35 m deepening of the thermocline in May 1997 against only 15 m in May 2014 (compare dotted and plain lines on Figures 3a and 3d). Further adding the 1997 WWE sequence onto the 2014 background (1997WWE experiment) allows retrieving a subsurface anomaly in May 2014 that is similar to that of May 1997 (not shown). Our set of sensitivity experiments hence demonstrates that the differences in subsurface temperature response between 1997 and 2014 can clearly be attributed to the different WWE forcing between the two periods.

The comparison above also highlights that the EEWP eastward displacement and subsurface temperature anomalies in the central and eastern Pacific are much weaker in mid-2014 than in mid-1997. This strongly suggests that the anticipated 2014 El Niño may not develop into a mature stage and should anyway be weaker than the one in 1997 because of its more limited development in summer, in relation with the absence of other strong WWEs after the March 2014 event. In order to test this assertion, we will now put these two periods into perspective in a more general context. To that end, Figure 4 provides a comparison of the heat content anomalies and EEWP displacement for all the El Niño events reported since 1980 and for the early part of 2014. The onset of the 1997 El Niño is associated with the largest equatorial heat content (Figure 4a) and eastward displacement of EEWP (Figure 4b). The 2014 EEWP early displacement was comparable to those of the strong 1982–1983 and moderate 1991–1992 and 2002–2003 El Niño events but does not particularly stand out anymore in July 2014, with a fast retreat back to its climatological position (Figure 4b). The equatorial Pacific heat content anomalies of early 2014 also largely overcame those observed during all other El Niño events including the strong 1982 El Niño, with the exception of the 1997 El Niño (Figure 4a), but this heat content is now dropping fast under the level of most other El Niños, with weak eastern Pacific anomalies.

This comparative analysis hence suggests that while the Pacific preconditioning in early 2014 was favorable to the onset of an El Niño with a potential of a strong El Niño, the absence of additional WWE occurrences after April 2014 now seems to exclude the possibility of a strong El Niño to develop and may lead to an aborted El Niño in austral summer 2014.

4. Discussion

The eastward displacement of the EEWP and subsurface temperature anomalies in the central and eastern Pacific were much weaker in July 2014 than in 1997. Sensitivity experiments performed with an ocean model indicate that the weak SST anomalies compared to 1997 can be attributed to the different WWE sequences during the two periods. Both periods are characterized by strong WWEs in January–March, but no subsequent WWEs occurred from April to July 2014 while there were WWEs in April and June 1997. Our results indicate that the absence of strong WWEs from April to July 2014 did significantly limit the eastward displacement of the EEWP in 2014, in contrast with 1997. Furthermore, easterly wind anomalies have developed since mid-2014, shifting the warm pool back into its climatological position. Therefore, the prospects of a major or even a "regular" El Niño event in 2014 now seem to vanish, as no strong ocean-atmosphere positive feedback currently develops.

Our simple analysis hence suggests that the growth rate of El Niño during its onset phase strongly depends on the detailed characteristics of the WWE activity during that period. It has been demonstrated that the probability of occurrence of WWEs depends on the EEWP location [*Vecchi and Harrison*, 2000; *Lengaigne et al.,* 2003; *Yu et al.,* 2003], WWEs being 3 times more likely to occur when the eastern edge of the warm pool is located to the east of the date line [*Eisenman et al.,* 2005]. Experiments using forced atmospheric global climate models [*Lengaigne et al.,* 2003; *Vecchi et al.,* 2006] have demonstrated that the enhanced envelope of intraseasonal wind activity at the onset of the 1997–1998 El Niño event did not only result from internal atmospheric variability but was partly a deterministic response of the atmosphere to SST forcing.

Our analysis clearly illustrates that the very similar location of the EEWP in the first months of 1997 and 2014 did not result in a similar sequence of subsequent WWEs. This fundamental difference for the fate of the subsequent El Niño conditions remains a key question to answer bearing in mind that the stochastic control of WWE occurrence may be large enough to strongly affect the ENSO cycle. These results echo the modeling results of *Lengaigne et al.* [2004a] who found that a strong displacement of the warm pool in the early part of the year could result in very different El Niño amplitude, depending on the characteristics of the internal atmospheric variability during El Niño onset phase. This sensitivity may therefore be an intrinsic limitation of the predictability of ENSO amplitude.

Acknowledgments

The cluster used for ROMS simulations at IRD Nouméa was funded through IRD's scientific computing effort project SPIRALES, the ANR "Cyclones & Climat," and GOPS (Grand Observatoire du Pacifique Sud). We thank Jérôme Lefèvre for his help on the ROMS code implementation. This work was supported by Agence Nationale de la Recherche (ANR) project METRO grant 2010-BLAN-616-01. The model data used here can be accessed freely upon request to Christophe Menkes. We thank two anonymous reviewers for their suggestions as well as comments from Mike McPhaden.

The Editor thanks two anonymous reviewers for their assistance in evaluating this paper.

References

Barnston, A. G., M. K. Tippett, M. L. L'Heureux, S. Li, and D. G. DeWitt (2011), Skill of real-time seasonal ENSO model predictions during 2002–11: Is our capability increasing?, *Bull. Am. Meteorol. Soc.*, *93*(5), 631–651, doi:10.1175/BAMS-D-11-00111.1.

Bjerknes, J. (1969), Atmospheric teleconnections from the equatorial Pacific, *Mon. Weather Rev.*, *97*(3), 163–172, doi:10.1175/1520-0493(1969)097<0163:ATFTEP>2.3.CO;2.

Bonjean, F., and G. S. E. Lagerloef (2002), Diagnostic model and analysis of the surface currents in the tropical Pacific Ocean, *J. Phys. Oceanogr.*, *32*(10), 2938–2954, doi:10.1175/1520-0485(2002)032<2938:DMAAOT>2.0.CO;2.

Boulanger, J.-P., C. Menkes, and M. Lengaigne (2004), Role of high-and low-frequency winds and wave reflection in the onset, growth and termination of the 1997–1998 El Nino, *Clim. Dyn.*, *22*(2–3), 267–280.

Cai, W., et al. (2014), Increasing frequency of extreme El Nino events due to greenhouse warming, *Nat. Clim. Change*, *4*(2), 111–116, doi:10.1038/nclimate2100.

Clarke, A. J. (2014), El Niño physics and El Niño predictability, *Annu. Rev. Mar. Sci.*, *6*(1), 79–99, doi:10.1146/annurev-marine-010213-135026.

Eisenman, I., L. Yu, and E. Tziperman (2005), Westerly wind bursts: ENSO's tail rather than the dog?, *J. Clim.*, *18*(24), 5224–5238, doi:10.1175/JCLI3588.1.

Fairall, C. W., E. F. Bradley, D. P. Rogers, J. B. Edson, and G. S. Young (1996), Bulk parameterization of air-sea fluxes for tropical ocean-global atmosphere coupled-ocean atmosphere response experiment, *J. Geophys. Res.*, *101*(C2), 3747–3764, doi:10.1029/95JC03205.

Fedorov, A. V., S. Hu, M. Lengaigne, and E. Guilyardi (2014), The impact of westerly wind bursts and ocean initial state on the development, and diversity of El Niño events, *Clim. Dyn.*, 1–21, doi:10.1007/s00382-014-2126-4.

Gebbie, G., I. Eisenman, A. Wittenberg, and E. Tziperman (2007), Modulation of Westerly Wind Bursts by sea surface temperature: A semi-stochastic feedback for ENSO, *J. Atmos. Sci.*, *64*(9), 3281–3295, doi:10.1175/JAS4029.1.

Harrison, D. E., and G. A. Vecchi (1997), Westerly Wind Events in the tropical Pacific, 1986–95*, *J. Clim.*, *10*(12), 3131–3156, doi:10.1175/1520-0442(1997)010<3131:WWEITT>2.0.CO;2.

Jullien, S., C. E. Menkes, P. Marchesiello, N. C. Jourdain, M. Lengaigne, A. Koch-Larrouy, J. Lefèvre, E. M. Vincent, and V. Faure (2012), Impact of tropical cyclones on the heat budget of the south Pacific Ocean, *J. Phys. Oceanogr.*, *42*(11), 1882–1906, doi:10.1175/JPO-D-11-0133.1.

Jullien, S., P. Marchesiello, C. E. Menkes, J. Lefèvre, N. C. Jourdain, G. Samson, and M. Lengaigne (2014), Ocean feedback to tropical cyclones: Climatology and processes, *Clim. Dyn.*, 1–24, doi:10.1007/s00382-014-2096-6.

Kanamitsu, M., W. Ebisuzaki, J. Woollen, S.-K. Yang, J. J. Hnilo, M. Fiorino, and G. L. Potter (2002), NCEP–DOE AMIP-II reanalysis (R-2), *Bull. Am. Meteorol. Soc.*, *83*(11), 1631–1643, doi:10.1175/BAMS-83-11-1631.

Kessler, W. S., M. J. McPhaden, and K. M. Weickmann (1995), Forcing of intraseasonal Kelvin waves in the equatorial Pacific, *J. Geophys. Res.*, *100*(C6), 10,613–10,631, doi:10.1029/95JC00382.

Lengaigne, M., J.-P. Boulanger, C. Menkes, G. Madec, P. Delecluse, E. Guilyardi, and J. Slingo (2003), The March 1997 Westerly Wind Event and the onset of the 1997/98 El Nino: Understanding the role of the atmospheric response, *J. Clim.*, *16*(20), 3330–3343.

Lengaigne, M., E. Guilyardi, J.-P. Boulanger, C. Menkes, P. Delecluse, P. Inness, J. Cole, and J. Slingo (2004a), Triggering of El Nino by Westerly Wind Events in a coupled general circulation model, *Clim. Dyn.*, *23*(6), 601–620.

Lengaigne, M., J.-P. Boulanger, C. Menkes, P. Delecluse, and J. Slingo (2004b), Westerly Wind Events in the tropical Pacific and their influence on the coupled ocean-atmosphere system: A review, in *Earth's Climate: The Ocean-Atmosphere Interaction*, *Geophys. Monogr. Ser.*, vol. 147, edited by C. Wang, S. P. Xie, and J. A. Carton, pp. 49–69, AGU, Washington, D. C.

Lian, T., D. Chen, Y. Tang, and Q. Wu (2014), Effects of westerly wind bursts on El Niño: A new perspective, *Geophys. Res. Lett.*, *41*, 3522–3527, doi:10.1002/2014GL059989.

Lopez, H., B. P. Kirtman, E. Tziperman, and G. Gebbie (2013), Impact of interactive westerly wind bursts on CCSM3, *Dyn. Atmos. Oceans*, *59*, 24–51, doi:10.1016/j.dynatmoce.2012.11.001.

McPhaden, M. J. (1999), Genesis and evolution of the 1997–98 El Niño, *Science*, *283*(5404), 950–954, doi:10.1126/science.283.5404.950.

McPhaden, M. J. (2012), A 21st century shift in the relationship between ENSO SST and warm water volume anomalies, *Geophys. Res. Lett.*, *39*, L09706, doi:10.1029/2012GL051826.

McPhaden, M. J., S. E. Zebiak, and M. H. Glantz (2006a), ENSO as an integrating concept in Earth, *Science*, *314*(5806), 1740–1745, doi:10.1126/science.1132588.

McPhaden, M. J., X. Zhang, H. H. Hendon, and M. C. Wheeler (2006b), Large scale dynamics and MJO forcing of ENSO variability, *Geophys. Res. Lett.*, *33*, L16702, doi:10.1029/2006GL026786.

Meinen, C. S., and M. J. McPhaden (2000), Observations of warm water volume changes in the equatorial Pacific and their relationship to El Niño and La Niña, *J. Clim.*, *13*(20), 3551–3559, doi:10.1175/1520-0442(2000)013<3551:OOWWVC>2.0.CO;2.

Reynolds, R. W., and T. M. Smith (1994), Improved global sea surface temperature analyses using optimum interpolation, *J. Clim.*, *7*(6), 929–948, doi:10.1175/1520-0442(1994)007<0929:IGSSTA>2.0.CO;2.

Seiki, A., and Y. N. Takayabu (2007), Westerly Wind Bursts and their relationship with intraseasonal variations and ENSO. Part I: Statistics, *Mon. Weather Rev.*, *135*(10), 3325–3345, doi:10.1175/MWR3477.1.

Shchepetkin, A. F., and J. C. McWilliams (2005), The regional oceanic modeling system (ROMS): A split-explicit, free-surface, topography-following-coordinate oceanic model, *Ocean Modell.*, *9*(4), 347–404, doi:10.1016/j.ocemod.2004.08.002.

Tollefson, J. (2014), El Niño tests forecasters, *Nature*, *508*(7494), 20–21, doi:10.1038/508020a.

Vecchi, G. A., and D. E. Harrison (2000), Tropical Pacific sea surface temperature anomalies, El Niño, and equatorial Westerly Wind Events*, *J. Clim.*, *13*(11), 1814–1830, doi:10.1175/1520-0442(2000)013<1814:TPSSTA>2.0.CO;2.

Vecchi, G. A., A. T. Wittenberg, and A. Rosati (2006), Reassessing the role of stochastic forcing in the 1997–1998 El Niño, *Geophys. Res. Lett.*, *33*, L01706, doi:10.1029/2005GL024738.

Wang, C., and J. Picaut (2004), Understanding ENSO physics: A review, in *Earth's Climate: The Ocean-Atmosphere Interaction*, *Geophys. Monogr. Ser.*, vol. 147, edited by C. Wang, S. P. Xie, and J. A. Carton, pp. 21–48, AGU, Washington, D. C.

Wang, W., M. Chen, A. Kumar, and Y. Xue (2011), How important is intraseasonal surface wind variability to real-time ENSO prediction?, *Geophys. Res. Lett.*, *38*, L13705, doi:10.1029/2011GL047684.

Yu, L., R. A. Weller, and W. T. Liu (2003), Case analysis of a role of ENSO in regulating the generation of westerly wind bursts in the western equatorial Pacific, *J. Geophys. Res.*, *108*(C4), 3128, doi:10.1029/2002JC001498.